CHAPTER 2

LITERATURE REVIEW

2.1 Basic of Ferroelectrics

The classification of crystals is based on their internal symmetry. In general, crystals can be divided into 32 point groups or crystal classes as shown in Figure 2.1. In the 32 point groups, 21 classes called noncentrosymmetric crystals which do not possess a center of symmetry. Twenty of these are piezoelectric. The only class that is not piezoelectric because of combined symmetry element, can not produce an electric dipole. An absence of a center of symmetry is significant for the presence of piezoelectricity. For piezoelectricity, this effect is linear and reversible ; piezoelectric material can develop a strain in response to an applied electric field and vice versa. Ten of 20 piezoelectric crystal classes named pyroelectric which are polar, because they possess a spontaneous polarization (permanent dipole moment) by virtue of their crystal structure. The pyroelectricity results from a change in polarization with temperature; the length of the polar axis varies with temperature.

Ferroelectric is a subgroup of the spontaneously polarized pyroelectric. This material can be oriented in equilibrium domain states by the application of an electric field. A non-centrosymmetric arrangement of ions in the unit cell which produces an electric dipole moment results in the spontaneous polarization. In ferroelectic, a domain is neighboring unit cells which tend to deform in the same direction and form a region. Domains which differ in the

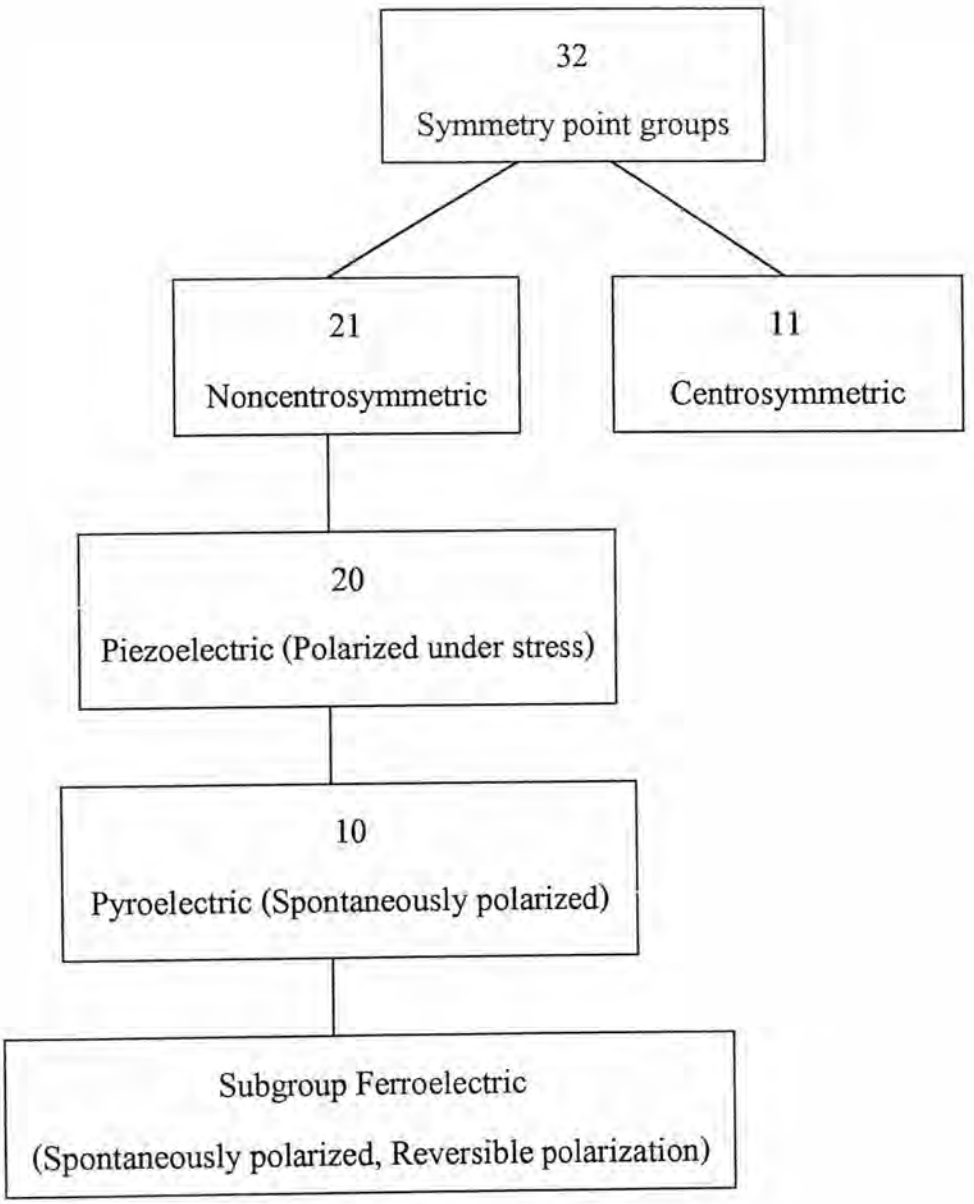

Figure 2.1 Interrelationship of piezoelectrics and subgroups on the basis of internal crystal symmetry (Buchanan 1991).

direction of spontaneous polarization can be switched by an applied electric field.

An ordinary structure of ferroelectrics is the ABO_3 perovskite-type structure as shown in Figure 2.2. Above Curie temperature, T_c or the transition temperature (for instances, 120°C for $BaTiO_3$ and about 490°C for $PbTiO_3$), the material is no longer ferroelectric thus reorientable and a spontaneous polarization is not shown. This high temperature phase is called the paraelectric phase, and the low temperature one is called ferroelectric phase which occurs below the Curie temperature. In this state, the cubic unit cell deforms into a non-centrosymmetric tetragonal, rhombohedral, or monoclinic phase (Lines and Glass 1977) due to the displacement of the B ion from its body-centered position. At the transition, a maximum in the dielectric permittivity, ε , is shown. Figure 2.3 shows the data of $BaTiO_3$ (Burfoot and Taylor 1979).

The hysteresis loop is the most distinctive part of ferroelectric materials. It presents the nonlinear polarization switching behavior as a function of an applied electric field. Figure 2.4 shows a typical hysteresis loop for a ferroelectric material. At low fields, domains remain randomly oriented. The polarization, P , is proportional to electric field, E , and the dielectric susceptibility , $\chi = P/\varepsilon_o E$, is constant. When the field is increased , dP/dE increases due to the orientation of domains with respect to the field direction. Also, domains grow in size at the expense of the other domains.

At very high fields, the polarization mechanisms saturate or approach P_{sat}. Then, the slope approaches zero. The polarization still remains eventhough the electric field is removed. At this stage, the polarization is named

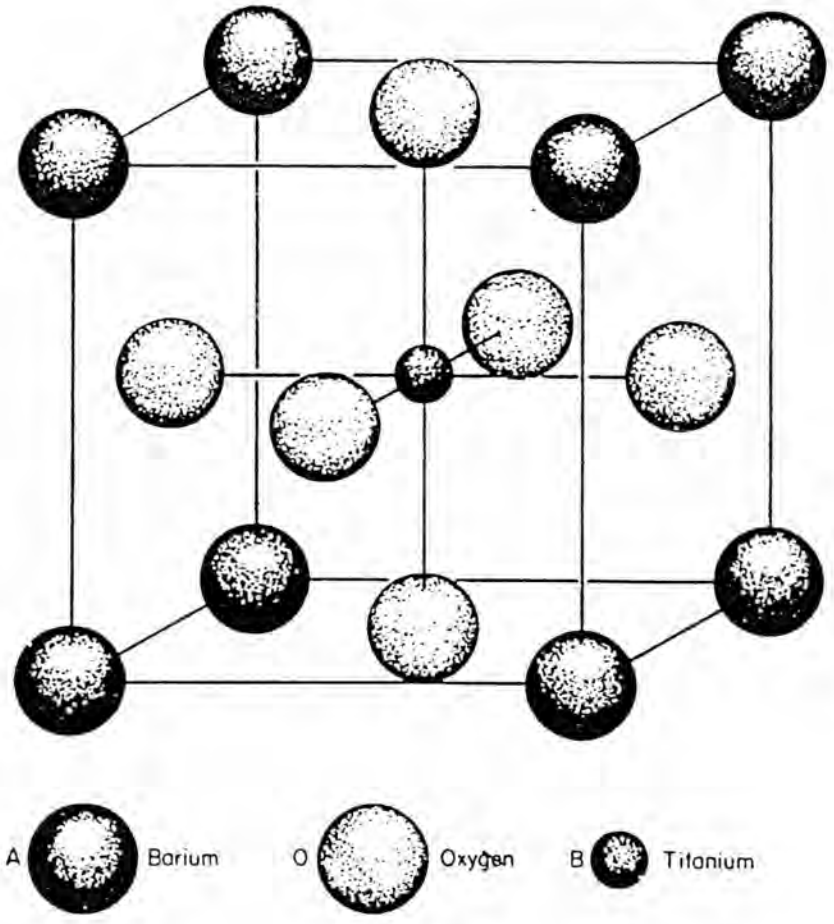

Figure 2.2 The perovskite unit cell of $BaTiO_3$ (after Jaffe et al. 1971).

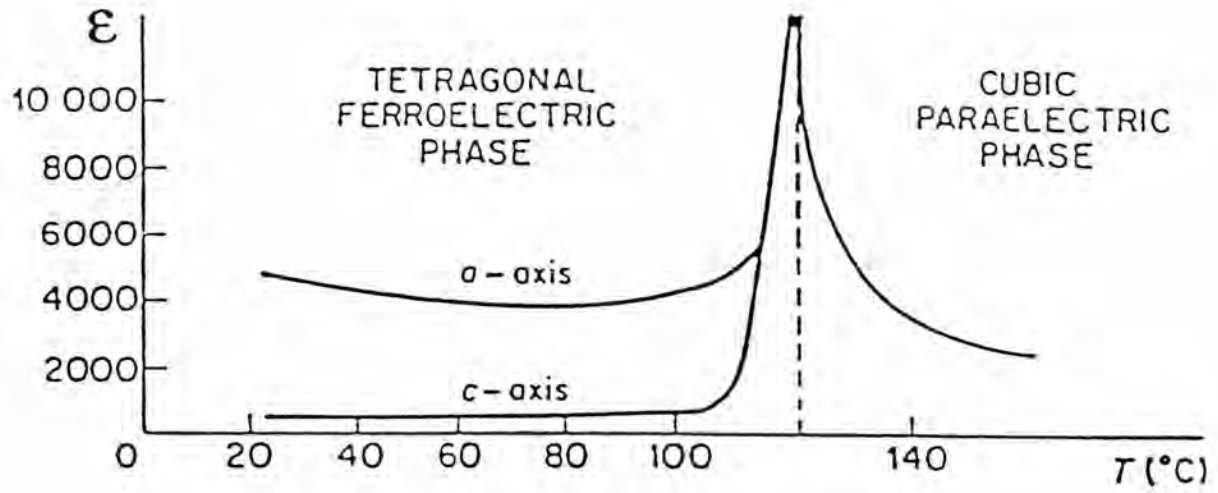

Figure 2.3 The Ferroelectric-paraelectric phase transition in a $BaTiO_3$ single crystal. The sharp increase of ε near the transition temperature is shown for measurements along the a and c-axes of $BaTiO_3$ (after Burfoot and Taylor 1979).

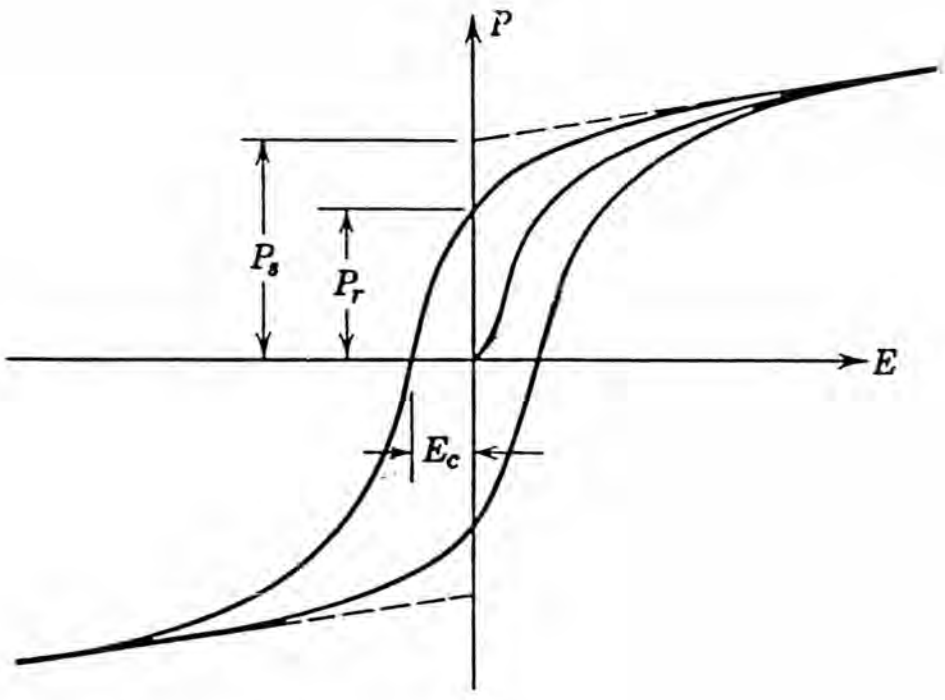

Figure 2.4 A typical hysteresis loop of a ferroelectric material. (from Kingery, Bowen and Uhlmann 1976).

the remanent polarization (P_r). As the field is reversed, the polarization decreases to zero. The polarization then changes direction when the field creates the saturation polarization in the opposite direction. The hysteresis loop is noticed upon cycling of the field because of the energy dissipated in the reorientation of domains.

2.2 Ferroelectric Applications

Valasek (1921) discovered the ferroelectric phenomenon in Rochlelle Salt(sodium potassium tartrate tetrahydrate, $NaKC_4H_4O_64H_2O$). Further developments in ferroelectric materials came in the early 1940s when ferroelectricity and the resulting high dielectric constant in $BaTiO_3$ were discovered for the first time. After that many other compounds in different structural families were found to have ferroelectric phases (Jaffe et al. 1971). In addition $BaTiO_3$, there are other compounds included $CdTiO_3$, $PbTiO_3$, $KNbO_3$, $BiFeO_3$, and $NaTaO_3$ and their solid solutions as well as tungsten-bronze compounds such as $(Sr,Ba)Nb_2O_6$ (Zheludev 1971 and Jaffe et al. 1955).

Ferroelectric materials were initially developed as bulk ceramics for industrial applications including ultrasonic cleaners, sonar transducers and capacitors (Jona and Shirane 1962). To date, these ceramic compounds, including barium titanate ($BaTiO_3$), barium strontium titanate (BST), lead zirconate titanate ($Pb(Zr,Ti)O_3$ or PZT), $SrBi_2Ta_2O_9$, $Bi_4Ti_3O_{12}$, $PbTiO_3$ and others have been fabricated in thin film forms (Scott et al. 1989 and Scott and Araujo 1989).

PZT is a good candidate ferroelectric which has wide applications in thin films. The phase diagram of the $Pb(Zr_xTi_{1-x})O_3$ system is shown in Figure 2.5 (Jaffe et al. 1971). At the morphotropic phase boundary composition where the ratio of $PbTiO_3$: $PbZrO_3$ is close to 1:1 and the materials exhibit superior ferroelectric and piezoelectric properties. This composition has a maximum number of 14 possible orientation states available; with 6 orientation states for tetragonal phase and 8 for rhombohedral phase (Jaffe et al. 1971). The proximity to such a phase boundary between the ferroelectric phases is believed to enhance physical properties in materials due to the increased ease of orientation during poling and polarization switching. Moreover, there is an increase in the dielectric constant and remanent polarization and reduction in the coercive field (Kwok et al. 1993). Thus, PZT composition at MPB has been widely used for memory and logic devices, especially in thin film form. It would be ideal to meet the requirements of low driving voltage, optimization of charge storage capacity and full polarization switched in a short time (< 200 nanoseconds) (Udayakumar et al. 1995).

Applications of ferroelectric thin films are summerized in Table 2.1. For electro-optic devices, advances in ferroelectric thin-film fabrication technology allow production of highly crystalline and optically transparent thin films. Particularly in waveguide application, a high degree of crystallographic orientation of the deposited film is required in order to minimize scattering at grain boundaries (Wilson and Hawkes 1983). More recent work has involved the lead-based ferroelectric such as PLT and PLZT (Takayama et al. 1987 and Baude et al. 1993).

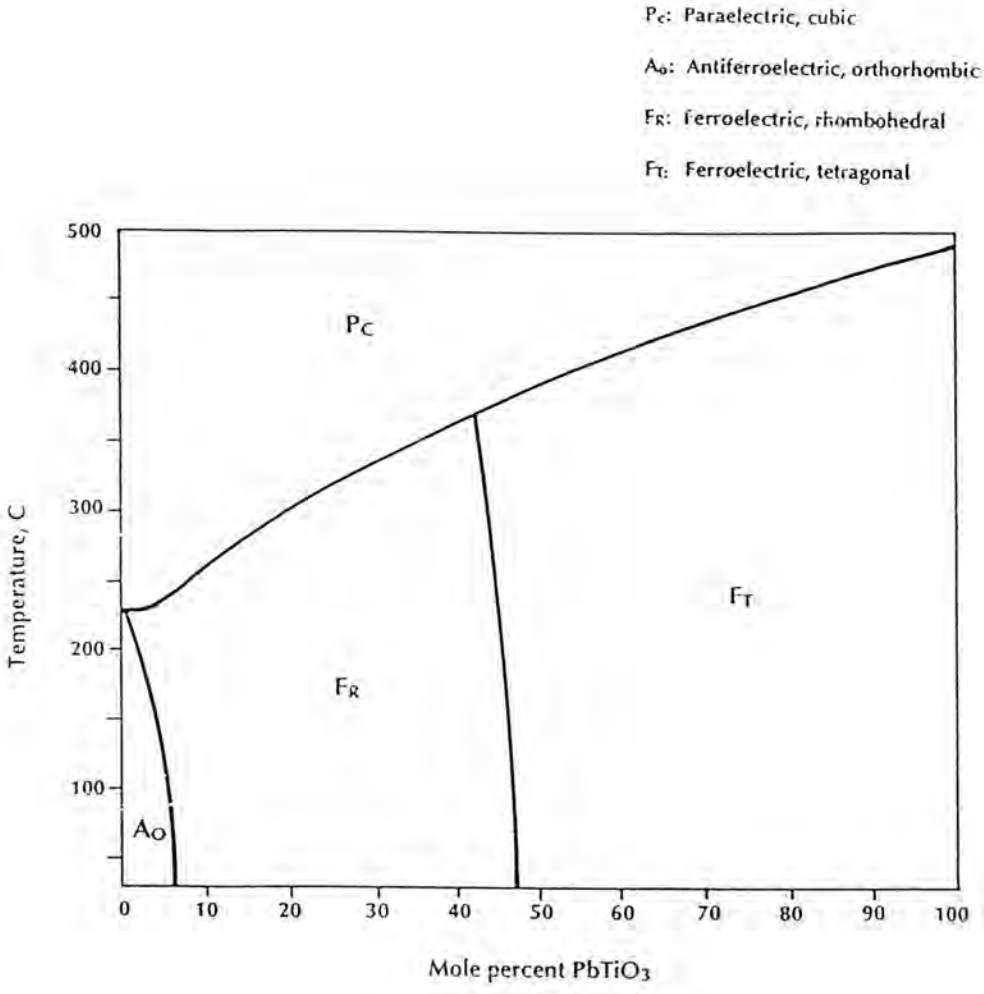

Figure 2.5 The phase diagram for the $Pb(Zr_xTi_{1-x})O_3$ system (after Jaffe et al. 1971).

Table 2.1: Application of Ferroelectric Thin Films (Swartz 1990).

Thin-Film Materials	Phenomenon	Applications
Perovskite Titanate		
$BaTiO_3$, $(Ba,Sr)TiO_3$	Dielectric	Capacitors
	Pyroelectric	Infrared (IR) detectors
$PbTiO_3$	Pyroelectric	IR detectors
	Piezoelectric	Acoustic transducers
$Pb(Zr,Ti)O_3$ (PZT)	Dielectric	Nonvolatile memories
	Pyroelectric	IR detectors
	Piezoelectric	Surface acoustic wave (SAW) substrates
	Electro-optic	Waveguide devices
$(Pb,La)(Zr,Ti)O_3$ (PLZT)	Pyroelectric	IR detectors
	Electro-optic	Waveguide devices
		Optical memories
		Display
Perovskite Niobates		
$Pb(Mg_{1/3}Nb_{2/3})O_3$ (PMN)	Dielectric	Capacitors
	Electro-optic	Waveguide devices
$LiNbO_3$, $KNbO_3$, $K(Ta,Nb)O_3$	Electro-optic	Waveguide devices
Tungsten-Bronze Niobates		
$(Sr,Ba)Nb_2O_6$ (SBN)	Pyroelectric	IR-detectors
	Electro-optic	Waveguide devices

At present, single crystal substrates such as quartz or $LiNbO_3$ are used to produce SAW devices (Ono and Takeo et al. 1995). SAW devices are commercially used as delay lines and filters in television and microwave communications (Wilson and Hawkes 1983, Sayer et al. 1992).

Lead-based compound films have also been investigated for pyroelectric detectors, such as intruder alarms, air conditioning controls and thermal imaging system (Whatmore 1991), and infrared sensors (Takayama et al. 1987). Ferroelectric thin films offer an advantage of flexibility in device design and avoid the high cost of single crystal fabrication. Recently, PZT thin films have also been used in application such as microelectromechanical systems (MEMS) (Chen et al. 1995 and Polla and Francis 1996) i.e. microsensors and microactuators (Sayer et al. 1992, Udayakumar et al. 1994).

For dielectric applications, it has become possible to fabricate ferroelectric thin film memories onto standard integrated circuits. Ferroelectric random-access memories (FRAMs) offer the following advantages for nonvolatile memories (Scott and Araujo 1989);

- very high speed read/erase/rewrite operation (30 nanosecond cycle time)
- low power requirements, compatible with existing integrated circuit (Si or GaAs circuit)
- very high density information storage (2 by 2 micrometer cell size)
- no applied field or voltage is required to maintain its remanent polarization (in other word, retention of memory when power is interrupted)

- extreme radiation hardness (ability to function and retain information when the memories are subjected to intense X-rays, particle fluxes of charged ions and neutrons)

Thus, ferroelectric random-access memories are expected to replace magnetic core memory, magnetic bubble memory systems, and electrically erasable read-only memory for many applications.

2.3 Deposition Methods

There are several deposition techniques which have been used to produce PZT films, including electron-beam evaporation (Oikawa and Toda 1976 and Castellano and Feinstein 1979), sputtering (Krupanidhi et al. 1983 and Okada 1978) , sol-gel (Fukushima et al. 1984, Budd et al. 1985, Udayakumar 1992 and Aungkavattana 1996), chemical vapor deposition (Okada et al. 1989 and 1990), rf magnetron sputtering (Krupanidhi et al. 1992, Takayama et al. 1987 and Adachi 1986), and laser ablation (Lee et al. 1993).

The selection of a suitable preparation technique is based on the final application of these ferroelectric films. The capital requirements for a compatible process are the followings:

1) strictly control of stoichiometry;

2) uniform deposition over a large area;

3) high deposition rate.

These techniques mentioned above are albitrarilly classified as physical and chemical techniques (Xu and Mackenzie 1992).

1) physical techniques

- evaporation (thermal, electron beam, laser etc.)

- sputtering (dc, rf, magnetron, ion beam, etc.)

2) chemical techniques

- CVD (chemical vapor deposition)
- MOD (metallo-organic deposition)
- Sol-gel

For chemical vapor deposition (CVD) (Ohring 1992), it is a deposition process by which gaseous stream of precursors containing the reactive constituents are consolidated onto a heated substrate where the reaction occurs. This method is possible to achieve good conformal coverage over complex-shape substrates with a good uniformity over large area. Moreover, CVD also allows stoichiometric control, the ability to fabricate a wide variety of high purity films and the possibility of easily accommodation dopant atoms (Okada et al.1989 and Sakashita et al. 1991).

However, CVD needs high vapor pressure and the gaseous precursors which is most hazadous and expensive. Reactant gaseous may be adversely affected the substrate material. For multicomponent oxides, it is a very complicated process. Furthermore, many experimental parameters must be optimized in order to obtain good quality films with required composition and uniformity such as the source delivery rate, the total pressure, and the deposition temperature.

Pulsed laser ablation (Lee et al. 1993) can be described as following steps:

1) Interaction of laser radiation with target and formation of plasma near the target;

2) Inertial expansion of plasma ions and other particles ablated from target;

3) Condensation of ablated material onto substrate surface and subsequent growth.

This method is simple and powerful for deposition of heterostructure and epitaxial thin film. The disadvantages of this method are the presence of microsized particles on the film surface, non-uniformity over large area, and the limited ability to scale up the process for industrial applications (Auciello and Ramesh 1996).

Sputtering methods, including magnetron, rf- and ion-beam sputtering are the methods whereby target materials are bombarded by high energy ions which liberate atom spicies from target to deposit on substrates. These methods can produce high quality ferroelectric thin films and are able to work with large scale processing for industrial applications. Depending on the features of the deposition method, either metallic or oxide targets can be employed. Moreover, low substrate temperatures for an epitaxial film, contaminate-free film and multi-element deposition is possible.

Nevertheless, rf sputtering is difficult to prepare large and dense ceramic targets, which are required for getting uniform layers over a large substrate (Sreenivas and Sayer 1988). Besides, some other technical problems related to the sputtering methods are the followings:

1) preferential sputtering of multicomponent oxide targets. To minimize this problem, extensive bombardment of the oxide target is used to stabilize the stoichiometry of the surface to that of the material;

2) a limited control over the composition of the films. Pb-based perovskite films are greatly affected by Pb incorporation into the films. The starting targets have to be Pb-rich target in order to compensate for any subsequent losses during the process;

3) the existence of negative ions during sputtering of oxide targets has been exhibited to bombard the growing film uncontrollably. The bulk stoichiometry, the growth morphology, and the crytalline perfection can be damaged (Sreenivas and Sayer 1988, Auciello et al.1996);

4) relatively low deposition rates.

For vacuum and electron-beam evaporation (Oikawa and Toda 1976 and Castellano and Feinstein 1979), it is possible to attain high deposition rate and relatively uniform films. However, the composition of the films tends to be non-stoichiometry due to the different vapor pressures from the different source materials (Roy et al. 1990).

2.4 Sol-gel Processing

Sol-gel processing has been extensively used to prepare amorphous and crystalline materials. The composition, precursors, handling and heat treatments are the factors need to be considered. In general, the sol-gel process is the synthesis of an organic network at low temperature by a chemical reaction in solution. This technique involves the transition characterized by a relatively rapid change from a liquid (solution or colloidal solution) into a solid (gel-like state).

Sol-gel technology can be divided into two types. The first is colloidal method. This method involves the colloidal suspension of solid particles in a liquid to form a sol. In order to stable the colloid suspensions, electrolytes such as acids, bases, or salts are added to establish the proper pH value. Consequently, these electrolytes will generate electric charges on the particle surface. Destabilization of sols leads to coagulation and formation of gels (Schmidt 1994). The second is polymeric method. This method involves the polymerization of organometallic compounds such as alkoxides to form a gel with three-dimensional network structure.

In this study, the sol-gel processing of oxide films is polymeric method carried out by the polymerization of alkoxide precursors. The important and typical precursors for producing the sol-gel solution are metal alkoxides, $M(O\text{-}R)_n$. This general composition consists of a metal atom, M , bonded through oxygen to one or more alkyl radical, R(CH_3, C_2H_5, etc), where n is the valence of the cation. The precursors are dissolved in a suitable organic solvent in order to get a solution. The solvent must be carefully selected so that a solution with high concentration of the required component is obtained (Yi and Sayer 1991).

In general, the sol-gel process involves the following steps:1) precursor (sol) formation, 2) hydrolysis, 3) polycondensation, 4) film or gel formation, 5) organic pyrolysis by low temperature heat treatment, and 6) densification and crystallization by annealing process.

The first step, the starting materials, metal alkoxides, are mixed in organic solvent to form a solution. In the gelation process, the transition from a

solution into a solid, involves the hydrolysis and condensation of alkoxides. The following step, pyrolysis involves the removal of residual by-products or organic compounds. Finally, a higher-temperature heat treatment is required to develop desired structure in the films. This can be accomplished by conventional furnace annealing (CFA) or by a rapid thermal annealing (RTA) technique.

The sol-gel process is a deposition technique that offers the advantage of molecular homogeneity, high deposition rate and excellent compositional control. Because of mixing components on nanoscale in the solution, it is easy to introduce trace elements (dopants) by adding them in the form of organometallic compounds, soluble organic or inorganic salts (Kwok, Desu and Vijay 1993).

In addition, the sol-gel process can be deposited at ambient condition; vacuum processing is not needed. Another advantage of the sol-gel process is inexpensive comparing to other deposition techniques. Materials can be produced in a variety of forms such as fine powders, thin films, monoliths and fibers. However, some drawbacks of the sol-gel process are excessive shrinkage that can cause cracking in fired films and the limitation in selection of some precursor materials.

2.4.1 The Role of Precursors

In the present time, metal alkoxides are used as the precursors for polymeric gel in sol-gel processing. These precursors are readily used with a suitable organic solvent, which is usually alcohol, in order to get a solution.

Moreover, they are able to converted into inorganic materials. The choice of an alkoxide can be considered by many factors including metal content, reactivity, availability, cost, sensitivity to moisture and decomposition temperature.

A compound with less organic content and high metal content is a proper precursor. Less organic content causes in less volumetric shrinkage during drying and annealing. Therefore, film has less tendency to crack. However, a compound with high metal content is usually much more reactive, it may be difficult to prepare a stable solution. Because of alkoxides with different alkyl groups, the reactivity usually increases in the order of methyl > ethyl > propyl > butyl > higher order alkyl groups (Kwok, Desu and Vijay 1993).

In the case of PZT, Ti and Zr methoxides and ethoxides are too reactive to prepare a stable solution. Ti and Zr propoxides and butoxides are still quite reactive, but they can be retarded their reactivities by using some chemical modifications. Then, they can be effectively used in sol preparation. Pb 2-ethylhexanoate has been used in some studies and Pb acetate is another metallorganic compound used as Pb precursor (Vest et al. 1989 and Yi et al. 1988). Moreover, all the precursor components should have decomposition temperatures similar to each other. Decomposition temperature in each case should be lower than the crystallization temperature. Especially in the case of PZT, it should be around 350°C or lower (Kwok, Desu and Vijay 1993).

2.4.2 The Gelation Process

There are two important reactions in polymeric gel formation. These reactions are partial hydrolysis followed by condensation polymerization. Polymerization steps via hydrolysis and condensation reactions are illustrated in Figure 2.6 (Budd 1986) according to these reactions (Yi and Sayer 1991):

$$M(OR)_n + H_2O \dashrightarrow M(OR)_{n-1}(OH) + ROH \qquad \text{(hydrolysis) (1)}$$

$$M(OR)_n + M(OR)_{n-1}(OH) \dashrightarrow M_2O(OR)_{2n-2} + ROH \qquad \text{(condensation) (2)}$$

$$M(OR)_{n-1}(OH) + M(OR)_{n-1}(OH) \dashrightarrow M_2O(OR)_{2n-2} + H_2O \qquad \text{(condensation) (3)}$$

The M-O-M network product is formed by polycondensation reactions as in equation (2) and (3) which alcohol and water are produced as by product. These reactions lead to the degree of gelation regarding to the appropriate amount of water. Other critical parameters need to be considered are viscosity, and rheological properties of solutions. Therefore, many applications of controlled hydrolysis to obtain a desired molecular structure and appropriate viscosity of the solution are used to improve spin ability and coating ability. In addition, the solute concentration, viscosity, and surface tension of the solution and the deposition technique determine the film thickness and uniformity.

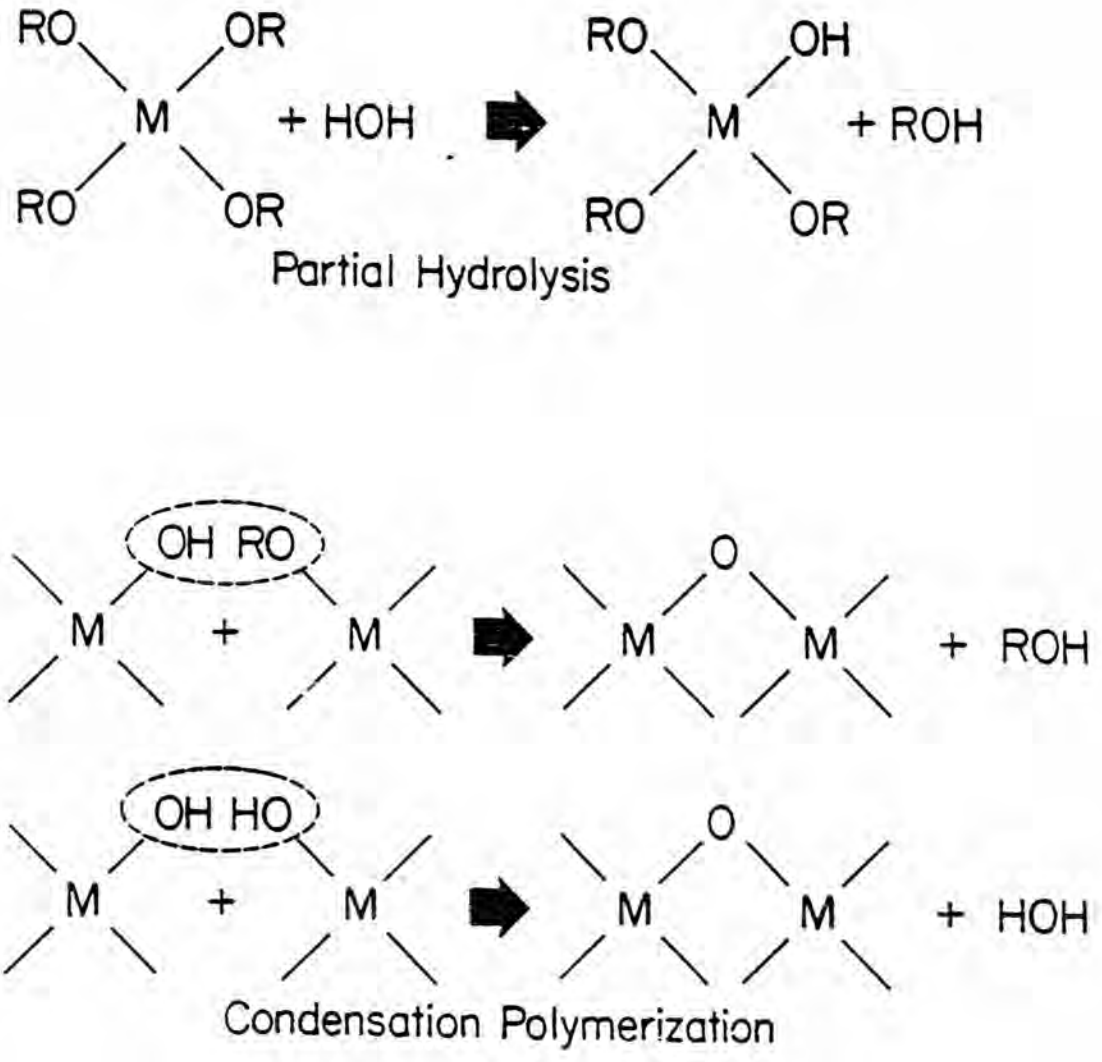

Figure 2.6 Polymerization steps via hydrolysis and condensation reactions (from Budd 1986).

2.4.3 Drying and Pyrolysis of the Gel

In this step, the drying temperature should be high enough to remove the free alcohol, the volatile organics, and water from the polymerized film. For PZT thin films, a range of drying temperature of 300°C to 400°C was selected in order to remove organic solvents. The critical problem in drying and pyrolysis is cracking built up from stresses. The gel consists of two phases, the network solid phase and connected pores filled with liquid phase. The liquid is removed from pores during drying process. The surface tensile stress and cracks begin to propagate which result from driving forces for liquid transport. In addition, the chemical or physical interaction of liquids with pore walls is a crucial cause of the capillary forces and the stress formation (Schmidt 1988).

When liquid evaporates from the surface of the porous body, the liquid in each pore at the pore surface will form a meniscus. The capillary pressure, P, of a wetting liquid in a cylindrical pore is related to the radius of meniscus by

$$P = 2V_{LV}\cos\theta/r \qquad (1)$$

where V_{LV} is the liquid/vapor interfacial energy, r is the radius of meniscus or the pore radius and θ is the solid-liquid wetting angle (Guppy and Atkinson 1992).

From the above mentioned, the capillary force and the variation of pore sizes cause in the stress concentration. This problem can be reduced by limiting the interaction between the liquid and the pore walls, and by decreasing the variation of pore sizes. These methods use surfactants, drying control chemical additives and hypercritical or supercritical drying.

A surfactant can decrease interfacial energy of the liquid/vapor (V_{LV}) in order to reduce the capillary force. Hypercritical drying involves using a pressure vessel at a temperature and pressure above the critical point of the solvent to remove either the original solvent or an exchanged fluid. The use of drying control chemical additives, including formamide, oxalic acid and others can provide larger and more uniform pores. Therefore, it can solve the problem of the cracking of gel films that occurs during drying process (Yi and Sayer 1991).

2.5 Sol-gel Processing of PZT Thin Films

The solution deposition of ferroelectric film has been developed over 15 years. PZT thin film fabricated by solution deposition was first reported by Fukushima et al. (1984). After that, other groups of researchers have investigated sol-gel PZT films from a variety of starting precursor chemistries. The most frequently used solution preparation may be grouped into three categories (Tuttle and Schwartz 1996);

1. Sol-gel process which used 2-methoxyethanol or alcohol as a solvent and metal alkoxide as a starting reagent (Budd et al. 1986 and Toughe et al. 1991).

2. Hybrid process which used chelating agents such as acetic acid or ethanolamine to reduce alkoxide reactivity (Yi et al. 1988 and Schwartz 1995).

3. Metallorganic decomposition (MOD) approaches which employed large water-insensitive carboxylate compounds (Vest and Xu 1989 and Haertling 1991).

The details on thin film processing are summerized and shown in Table 2.2. Sol-gel route by Budd et al. (1986) has been extensively followed by many groups of researchers including Udayakumar (1992), Gibbons (1995), Aungkavattana (1996) and this study. The advantages of the 2-methoxyethanol process are the following:

1. To offer controllable and reproducible chemistry
2. Stock solution has long shelf life (non-hydrolyzed solution exhibits minimal aging effects).

2.6 Crystallization of PZT Thin Films

Generally, the as-deposited films are in amorphous stage and retain some organic solvents. Amorphous films that have been pyrolyzed were subsequently heated to annealing temperatures of 500-700°C for crystallization at heating rates of 5°C/minute to 200°C/second, in case of using conventional furnaces and rapid-thermal-annealing furnaces (RTA) (Reaney et al. 1994). During crystallization, sol-gel PZT films first crytallized into an intermediate phase or pyrochlore-like phase before transforming to the perovskite structure (Tuttle et al. 1992, Hsueh and McCartney 1991, Lakeman et al. 1995).

A single-phase perovskite microstructure is highly desirable regarding to its remarkable ferroelectric and dielectric properties. The pyrochlore-like phase is a nonferroelectric phase and has a much lower dielectric constant ($K \sim 50$) than the perovskite phase ($K \sim 1000$). Thus, the residual of second phase in the films results in deterioration in the values of electrical properties. Pyrochlore (or Pb-Ti fluorite) is a nanocrystalline intermediate phase normally formed before transforming to perovskite phase at temperature as low as 490°C

Lead	Titanium	Zirconium	Solvent	Additive	Reference
Alcohol					
acetate trihydrate	isopropoxide	n-propoxide	methoxyethanol	water	Budd et al. (1986)
ethoxide	n-butoxide	n-butoxide	acetylacetone /ethyl alcohol	water	Toghe et al. (1991)
Acid/Water					
acetate trihydrate	isopropoxide	n-propoxide	propanol / acetic acid	water	Yi et al. (1988)
acetate trihydrate	isopropoxide	n-butoxide	methanol /acetic acid	water	Schwartz et al. (1995)
MOD					
acetate trihydrate	acetyacetonate	acetate	water	water	Haertling (1991)
2-ethylhexanoate	di-methoxy-di-neodeconate	decanoate	xylene	no	Vest et al. (1989)

Table 2.2 Precursors and solvents for solution deposition.

(Hu et al. 1993). Moreover, an intermediate phase can be stable up to a high temperature (Castellano and Feinstein 1979).

2.6.1 Intermediate Phase or Pyrochlore-like Structure

The name "pyrochlore" represents a family of phase isostructure to the mineral pyrochlore, (NaCa)(NbTa)O_6F/(OH). The general formula of oxide pyrochlore is written as $A_2B_2O_6O'$ with four non-equivalent kinds of atom that can be described in two ways (Subramanian et al. 1983);

1. Fluorite structure

Figure 2.7a shows that A and B cations form a face center cubic array and the anions are located in the tetrahedral interstices of the cation arrays. The face center A and B cations are located in alternate [110] rows in every other [001] plane and in alternate [110] rows in the other [001] plane subsequently three kinds of tetrahedral interstice anions are formed. The 48f positions have two A and B near-neighbours, the 8a positions which are vacant have four B near-nieghbours and 8b positions have four A near-positions. This type of structure occurs only in the compounds containing large B cation such as Zr^{4+}.

2. A three dimentional network structure of corner linked BO_6 octahedral

Figure 2.7b shows that A cations have 8 fold co-ordination (six O ions (48f) from the BO_6 octahedra, and two O' atoms (8b)). Each A cation is at the center of a hexagonal ring of six O atoms while a pair O' atoms are normal to the mean plane of this hexagonal ring. This structure is consistent with the

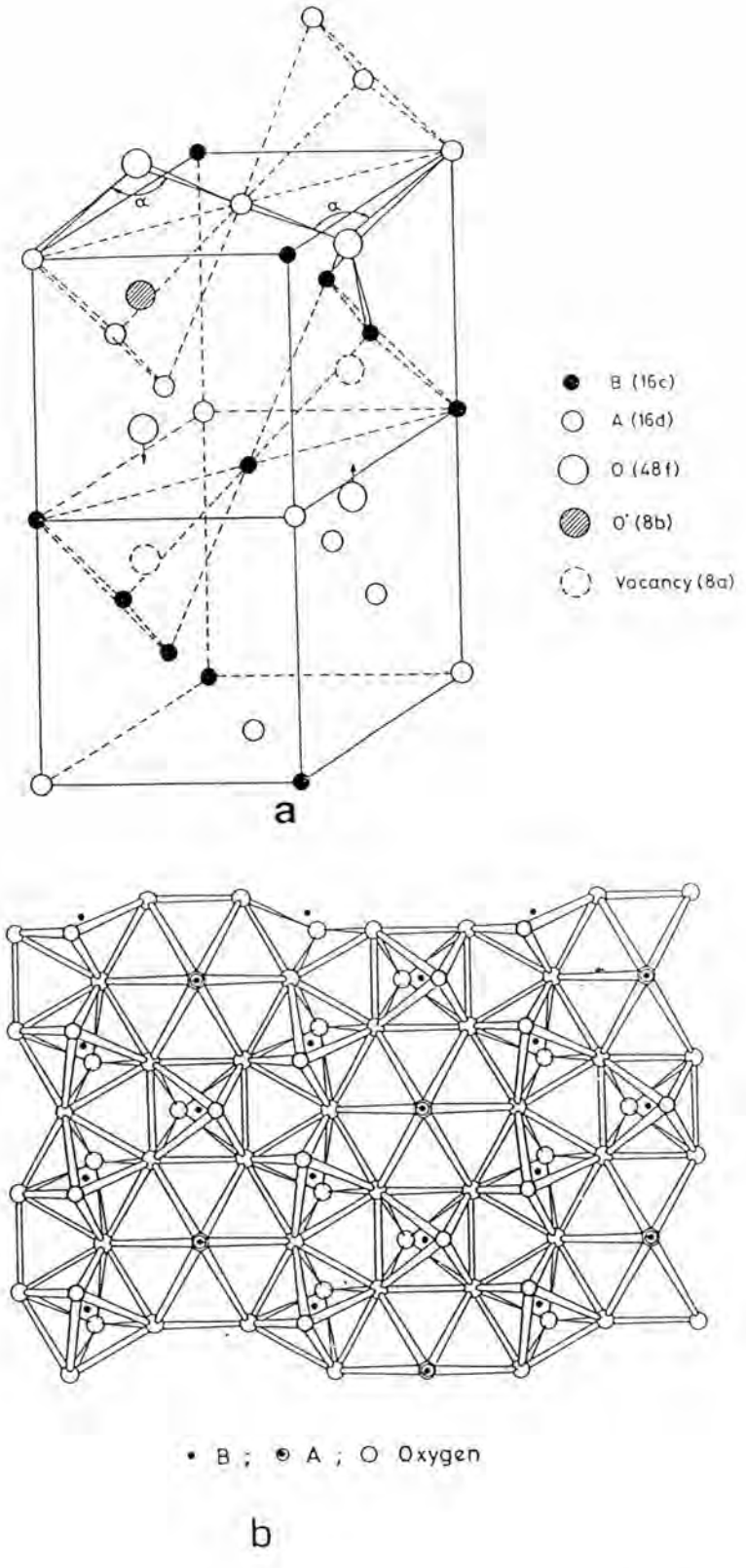

Figure 2.7 Pyrochlore structure (a) the fluorite structure and (b) BO_6 octahedral network (Subramanian et al. 1983).

occurrence of defect pyrochlores of type □AB_2O_6□ and $A_2B_2O_{7-x}$□$_x$ (□vacancy) since the BO_6 octahedra network forms the backbone of the structure. This structure is generally called a face center pyrochlore structure with higher symmetry in the case of PZT.

The real structure of the intermediate or pyrochlore-like structure which form forms prior to perovskite phase in PZT is still under discussions by many groups of researchers. The observed intermediate phases were found to be either pyrochlore or fluorite-type structure.

Pyrochlore is well known to exhibit wide ranges of stoichiometry which is a typical nonstoichiometric oxide. Ideally, pyrochlore structure is written as $A_2B_2O_7$ (Subramanian et al. 1983). The oxygen content may be as low as O_6, $Pb_2Ti_2O_6$ (Bursill 1994). The presence of excess or deficient PbO, Pb^{4+} and/or oxygen stoichiometry will all affect the formation of more or less stable pyrochlore phase. In oxidizing condition, a more stable pyrochlore, formulated as $Pb^{2+}_{1-x}Pb^{4+}_{1+x}(Zr^{4+}Ti^{4+})_2O_{7-x}$, forms. Consequently, the formation of perovskite phase slows down. In less oxidizing condition, a metastable pyrochlore, $Pb^{2+}_2(Zr^{4+}Ti^{4+})_2O_6$ forms and then fully converses to perovskite phase (Brooks et al 1994).

The observation related to Pb valency stated by Brooks et al. (1994) corresponded with the observation by Fox and Krupandhi (1994). The oxygen deficient films fully transformed to a perovskite phase, while pyrochlore formed when excess oxygen was present.

Hsuch and McCartney (1991) performed a microstructural investigation and local chemistry of films formed by two different precursor routes (acid- and base-modified stock solution) by transmission electron microscope (TEM) and energy dispersive detection systems (EDS). Their analysis also indicated that the perovskite phase morphology for PZT 54/46 films was large circular or a rosette structure. It was believed that the rosettes PZT grew from a pyrochlore matrix. This rosette phase also found in the study of Tuttle et al (1992) by using an optical microscope. It presented that the film fired at 550 to 600°C appeared diphasic. At higher annealing temperature, the average rosette diameter was smaller.

Moreover, semiquantitative EDS analysis in base-modified PZT films indicated that the pyrochlore regions and the PZT rosettes still had similar composition. In acid-modified PZT film, EDS analysis showed that the pyrochlore was Zr rich and Pb and Ti deficient, while perovskite exhibited a Zr-deficient nonstiochiometry. However, the observation of Carim (1991), transmission electron diffraction and EDS were used to determine the rosettes, which was roughly Pb/Zr/Ti $\approx$ 2/1/1 in all films.

Kwok and Desu (1992) also used transmission electron diffraction and X-ray diffractometer (XRD) to study pyrochlore to perovskite phase transformation. The comparison of d spacings observed by both ways showed a very good agreement. The d spacings measured from the spot pattern matched very well with XRD results. They also used transmission electron diffraction to examine that the perovskite particles grew on the pyrochlore phase. Therefore, they identified the fine grain structure as pyrochlore phase. This observation

was similar to the results of the studies by Chang and Desu (1994), Griswold et al. (1995), Brooks et al. (1994) and Heuch and McCartney (1991).

Chang and Desu (1994), using scanning transmission electron microscope (STEM) and backscattering electrons, showed the similarity in an image contrast between the interior perovskite grain and the surrounding pyrochlore phase. This indicated that compositions of both phases were almost the same. Moreover, Tuttle et al. (1994) found that Zr to Ti stoichiometry strongly influenced microstructure. The microstructure of film at near MPB composition consisted of two nanophases (pyrochlore and amorphous phase) and rosette perovskite phase. While Ti content increased, the perovskite phase increased, grain size became smaller, and the amount of pyrochlore phase decreased.

Eventhough study of Kwok et al. (1992) reported that the nanocrystalline phase which forms prior to crystallization of perovskite phase has frequently been described as a pyrochlore phase. Wilkinson et al. (1994) suggested that the intermediate phase had a fluorite structure with a lattice parameter, a $\sim$ 0.525 nm, rather than pyrochlore-like structure. The argument was upon the absence of superlattice reflections in diffraction data and the tendency for Zr to adopt co-ordination number higher than 6.

Lakeman et al. (1995) used TEM, EDX and Fourier transform infrared spectroscopy (FTIR) to study on phase evolution of PZT thin films. Their results were in agreement with those by Wilkinson et al. (1994). The selective area diffraction patterns (SADP) for the nanocrystalline phase could be indexed as a cubic fluorite structure with lattice parameter a $\sim$ 0.51 nm. The presence of

superlattice reflections for the related pyrochlore structure with a ~ 1.05 nm was not observed in their study. However, FTIR study indicated that both TiO_6 and ZrO_6 octahedra were formed during hydrolysis and low-temperature heat treatment whereas the fluorite structure required 8-fold co-ordination around cations. They noted that a disordered fluorite solid solution could be crystallized at low temperature and then transformed to an ordered pyrochlore structure on extended heat treatment at temperature below the perovskite crystallization temperature.

Two processing techniques have been investigated in order to reduce the pyrochlore phase formation for the lead-based ferroelectric thin layers (Dang and Gooding 1995 and Kaewchinda 1998);

1. Additions of excess Pb in solution
2. RTA (Rapid Thermal Annealing)

2.6.2 Additions of Excess Pb in Solution

It is well known that PbO additions are traditionally used with bulk PZT ceramics to improve densification behavior and electrical properties (Levett 1963). Although, film processing temperature is lower than bulk ceramic temperature, any locallized PbO deficiencies resulted from PbO volatility can enhance the formation of intermediate phase.

Study of Klee et al. (1992) was reported that the formation of perovskite may be attributed to the formation of lead oxide from the perfect pyrochlore state and an amount of Pb excess. Schematically, this corresponds to

$$\underset{}{\text{Excess Pb}} + \underset{\text{(perfect pyrochlore state)}}{Pb_2(Zr/Ti)_2O_7} \longrightarrow \underset{}{\text{Excess PbO}} + \underset{\text{(defect-pyrochlore)}}{Pb_2(Zr/Ti)_2O_6}$$

The obtained intermediate (defect-pyrochlore) phase then transformed to perovskite phase without any diffusion.

Many of the studies on sol-gel PZT thin film (Tuttle et al. 1990, Roy et al. 1990, Carim et al 1991 and Polli and Lange 1995) have reported that the intermediate phase can be transformed to the perovskite phase by increasing the Pb content, or increasing the annealing temperature and times (Kwok et al. 1990 and Krupanidhi et al. 1992). Thus, this technique is used in order to compensate for Pb-loss during annealing and lead to better electrical properties.

2.6.3 Rapid Thermal Annealing (RTA) for Ferroelectric Thin Films

To date, RTA has been adapted to crystallized ferroelectric thin films. RTA furnace allowed control of rapid and linear heating rates from 10°C/s to 200°C/s with accurate holding conditions (Singh 1988). Employment of RTA in the ferroelectric thin films was first reported by Udayakumar et al. (1990). Many of the ferroelectric film applications demand successful integration of the films into semiconductor devices. It can reduce either the annealing temperature and time in order to avoid defects at the interfacial film-substrate (Sreenivas et al. 1990).

A high temperature and long holding time could occur not only serious diffusion between substrate and films but also elemental loss at the surface and

damaging the components of the existing device. Such devices could not stand intensive heat treatment (e.g. 650°C for 1 hour) and they tend to undergo interface reactions or show degradation (Vasant Kumar et al. 1991 and Hu et al. 1992).

Moreover, the role of ramp rate in RTA was significant in phase transformation to perovskite. At slower ramp rates, the PbO which was necessary to complete the transformation had volatiled during heat treatment. Thus, with a ramp rate less than 50°C/s, the bulk and film surface showed the undesired pyrochlore phase (Griswold et al. 1995).

Tuttle et al. (1990) fabricated and characterized chemically derived PZT (53/47) films prepared with different excess Pb additions and fired at different heating rates. Excess Pb additions (up to 5 mole%) and fast heating rates increased the perovskite content and improved ferroelectric properties of films fired at 600°C. Films fabricated with a heating rate of 3°C/min had a remanent polarization of 5 $\mu C/cm^2$ whereas films heated at 50°C/min had a remanent polarization of 9 $\mu C/cm^2$. These polarizations are consistent with the perovskite content of the films.

Hu et al. (1993) reported that the perovskite phase formation nucleation kinetics appeared to be more effective with RTA process. It may be attributed to the fast rising in temperature and reaching the equilibrium. During the formation of perovskite phase, fast rise and decrease in temperature may be responsible for the absense of several secondary phases, since it did not give enough time for second phase to grow. In addition, RTA can minimize the thin

film-substrate interface reactions and Pb losses. Moreover, this process can also reduce the post-deposition annealing thermal budget.

2.7 Thick Ceramic Coatings

In general, ceramic films of up to 0.5 μm are deposited in a single layer. The required thickness is achieved by multiple coatings. At present, such film thickness achieved has been the main limitation in sol-gel processing, since it is difficult to fabricate crack-free thicker films. This restriction limits the potential applications because there are many piezoelectric applications which require thickness greater than 10 μm.

A new sol-gel based composite technology has proved to be success in fabrication of thick film without any cracking. Moreover, the advantages of composite material are simple, relatively inexpensive and enable to coat complex geometry. In addition, a wide range of film thickness has been fabricated on a variety of substrate materials (5-200 μm) (Barrow 1997).

Thick films are made by dispersing ceramic powders into a sol-gel solution. This resulting composite material or paste composition will consist of a ceramic thin-film matrix with bulk ceramic powders dispersed throughout. The paste composition can be coated onto a substrate by many ways such as spin-, dip coating or painting. Then, as-coated films are fired and annealed in the same way to conventional sol-gel, which is usually lower annealing temperature than bulk ceramics.

The thick films do not crack during processing which can be ascribed to two ways (Barrow et al. 1995);

1. Sol-gel solution is bonded strongly with ceramic particles. Thus, the film will not crack during processing.

2. Less shrinkage occurs since the percentage of sol-gel solutions of fabricated films are decreased.

The screen printing method is a coating process that has been used to form thick film patterns of metals and wide variety of ceramic materials. The advantages of screen printing method are versatile and inexpensive. In addition, this method can be applied to most any imaging requirement and it is very useful in an electronics market (Duccilli 1993). Multiple printings are used to produce the desired combination of electrical components.

2.7.1 Screen Printing Process

Generally, a thick film circuit comprised layers of special inks (or paste) is deposited onto a substrate. One of the methods of film deposition is screen printing which is used to produce a thick film circuit. Typical thick film screen materials consist of a fine woven mesh of stainless steel, nylon or polyester, mounted under tension on a metal frame. The circuit pattern can be formed photographically by coating the mesh with an ultra violet (UV) sensitive emulsion. The ink is placed on the opposite side of screen. A squeegee traverses the screen under pressure and forces the ink through the open areas of the mesh. Then, the circuit pattern is left on the substrate. Figure 2.8 shows the constituent parts of a screen printer (Prudenziati 1994).

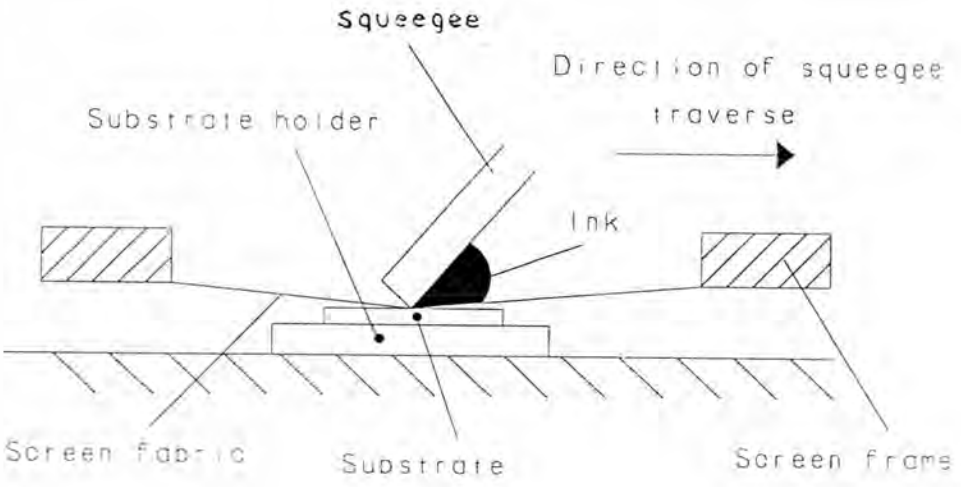

Figure 2.8 The schematic parts of a screen printer.

The primary factors that affect print thickness are amount of solid content and the screen mesh count (Cote' and Bonchard 1988). For general purpose work, a mesh count might be 200 strands per inch. The mesh opening depends on the mesh count and the filament diameter. A cross-section of a mesh and difinition terms are shown in Figure 2.9. The percentage open area of mesh is defined as follows:

$$\text{Percentage open area} = 100A^2/(A+D)^2$$

Where A is the mesh aperture and D is the filament diameter.

2.7.2 Fluid Rheology

In screen printing technique, the paste composition is forced through a stencil screen onto the substrate belowed. An important property of the paste for printing is its viscosity. The paste must be shear thinning (pseudoplastic) and thixotropic. So, it will flow readily through the apertures of the screen and the print blocks will form a monolitic film (Reed 1995). Pseudoplastic and thixotropic are the possible rheological properties behaviours of materials as seen in Figure 2.10 (Prudenziati 1994).

Figure 2.10 shows the relationships between the shear stress VS. shear rate of fluids. Shear stress (σ_s) is the pressure (or force per unit area measured in Pascal, Pa) applied to a viscous fluid to cause its movement on a plane. Shear rate (r_s) is the velocity (v) of the relative shift of two planes, separated by fluid for a distance (x), divided by the distance itself ($r_s = \delta v/\delta x$). The viscosity of the fluid η is ratio between shear stress and shear rate, i.e. $\eta = \sigma_s / r_s$ (Prudenziati 1994 and Reed 1995).

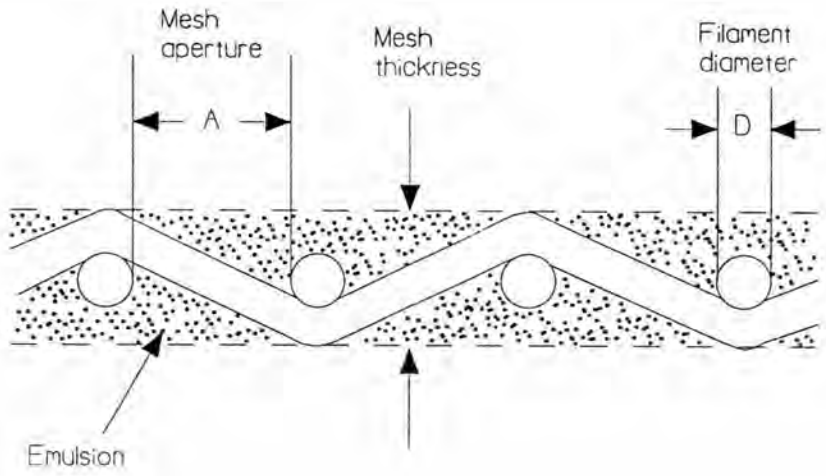

Figure 2.9 Cross-section of a screen mesh.

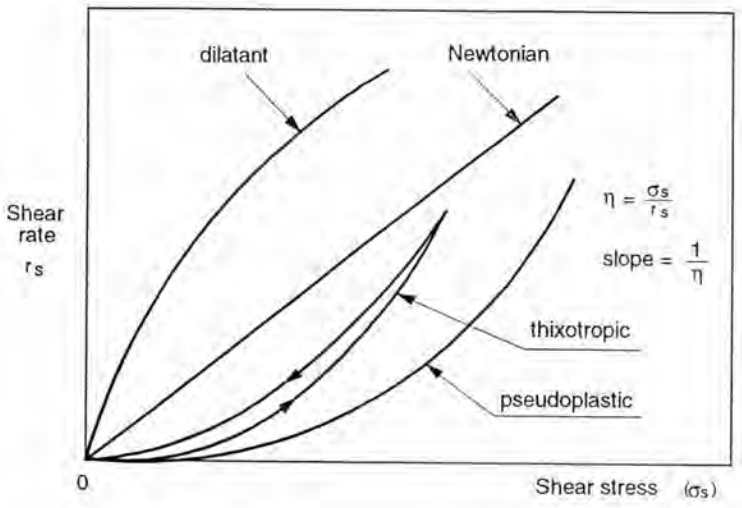

Figure 2.10 Response of fluids to shear (Prudenziati 1994).

2.7.3 Firing Process

Particle size of powders strongly affects the characteristics of the fired films, e.g. in terms of sinterability and densification. A mean size is usually lower than 5 μm, sometimes in the range from 0.1 to 0.5 μm. In addition, firing process must be carefully controlled to obtain crack-free films. From the above mentioned, paste composition is composed of solvent, polymer and inorganic powders. During drying and firing process, the solvent evaporates at 150°C. The polymer decomposes at about 150-500°C. Thus, the heating rate from 150 to 500°C is much slower rate than in thin film processing. The rate is typically limited to 50-85°C/minute to ensure that all organic residual is removed and no carbon entrapment occurred (Cote′ and Bonchard 1988).